Synthesis of Heterograft Copolymers with a Semifluorinated Backbone by Combination of Grafting-through and Graftingfrom Polymerizations

Jeonghyeon Lee, Gérald Lopez, Bruno Ameduri, Myungeun Seo

Synthesis of Heterograft Copolymers with a Semifluorinated Backbone by Combination of Grafting-through and Grafting-from Polymerizations

Jeonghyeon Lee,[1] Gérald Lopez,[2] Bruno Améduri[2*] and Myungeun Seo[1,3,4]*

[1]Graduate School of Nanoscience and Technology, Korea Advanced Institute of Science and Technology (KAIST), Daejeon 34141, Korea

[2]Institut Charles Gerhardt Montpellier, Université de Montpellier, CNRS, ENSCM, Place Eugene Bataillon, 34095 Montpellier, France

[3]Department of Chemistry, KAIST, Daejeon 34141, Korea

[4]KAIST Institute for Nanocentury, KAIST, Daejeon 34141, Korea

*To whom should be addressed: bruno.ameduri@enscm.fr (B. A.); seomyungeun@kaist.ac.kr (M. S.)

Abstract

We report that an alternating semifluorinated copolymer of chlorotrifluoroethylene (CTFE) and vinyl ether (VE) is an attractive platform for the synthesis of heterograft copolymers consisting of two distinct side chains. The radical terpolymerization of CTFE with PLA-tethered vinyl ether (PLAVE) synthesized by ring opening polymerization and isobutyl vinyl ether (IBVE) as a spacer produced PLA-grafted fluorinated copolymer via a "grafting-through" manner. Two PLAVEs with different molar masses (2 and 10 kg mol^{-1}) were successfully incorporated, and the grafting density could be controlled by varying the [PLAVE]/[IBVE] initial molar ratio. From the chlorine atoms in the CTFE repeating units, atom transfer radical polymerization (ATRP) of styrene was further employed to grow PS side chains following a "grafting-from" mechanism per each (CTFE-*alt*-VE) repeating unit pair. First-order kinetics was observed for the styrene polymerization and supported controlled growth of PS. The resulting heterograft copolymers possessed regularly spaced PS chains and statistically distributed PLA chains on the backbone, generating a nanoscopic disordered morphology via microphase separation driven by incompatibility between PLA and PS. By copolymerization of styrene and divinylbenzene (DVB) in neat ATRP condition, a cross-linked polymer monolith with the disordered bicontinuous morphology could be also prepared via polymerization-induced microphase separation. The cross-linked precursor was converted into a mesoporous polymer with pore size of 3.7 – 10.4 nm by removal of PLA. The mesopore size was tunable by adjusting the PLA molar mass and styrene/DVB molar ratio.

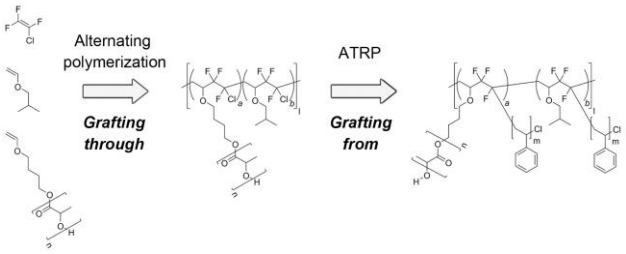

For Table of Contents use only

Introduction

Alternating radical copolymerization of vinyl monomers with fluorinated monomers provides a fascinating route to functional fluorinated copolymers. While retaining excellent properties of fluorinated polymers to some extent including low surface energy (hydrophobicity and oleophobicity), low adhesion, thermal stability, chemical inertness, and material properties of the copolymers can be widely tunable by incorporating non-halogenated repeating units in an alternating manner.[1] For example, electron-deficient chlorotrifluoroethylene (CTFE) can be well copolymerized with electron-rich monomers such as ethylene and vinyl ethers (VEs).[2,3] One kind of P(CTFE-*alt*-VE) has been commercialized by AGC company as paint under the Lumiflon® brand name.[4] These monomers are known to form an acceptor-donor charge transfer complex during polymerization which lowers an activation energy for an alternating propagation. This alternating tendency is relatively independent from the pendent alkoxy group of VE. Therefore, various VEs with a wide range of functional groups,[5] such as cyclocarbonate,[6] triazole,[7] imidazole,[8] azido,[9] and oligo(ethylene oxide)[10] were synthesized for various applications.

PCTFE can be also functionalized by the post-polymerization modification.[1] Although fluorinated polymers are often considered as relatively inert, chlorine on the PCTFE backbone is susceptible to undergo a variety of chemical modifications while keeping the advantages of fluorinated (co)polymers.[1] As a result, introducing ester, alcohol, and aromatic groups into PCTFE backbone was demonstrated by using diverse metal carbonyl as catalyst.[11] Feasibility of "grafting-from" polymerization via atom transfer radical polymerization (ATRP) was also reported by utilizing the chlorine as an initiator. Graft copolymers containing side chains of polystyrenics, polyacrylates, and polymethacrylates have been successfully synthesized.[12-17]

P(CTFE-*alt*-VE) provides an interesting platform for synthesis of heterograft

copolymers by combination of "grafting-through" and "grafting-from" approaches. VE macromonomers can be synthesized by modifying the pendent group, and copolymerized with CTFE to produce a graft copolymer. ATRP using the chlorine on the P(CTFE-*alt*-VE) as the initiating sites can graft another polymer chain to yield the heterograft copolymer. Chemically distinct polymers synthesized via different polymerization mechanisms can be grafted on a single polymer backbone, drastically enriching possible combinations and offering possibilities of microphase separation induced by side chain incompatibility.[18-20] Notably, amphiphilic heterografted molecular brushes containing poly(ethylene oxide) and poly(*n*-butyl acrylate) side chains have been synthesized following this strategy.[21,22] The hydrophilic and hydrophobic side chains effectively stabilized oil/water interface by intramolecular segregation, where the backbone was located at the interface as a boundary. A semifluorinated backbone provided by P(CTFE-*alt*-VE) can add more diversity to the microphase separation and interfacial behavior by taking advantages of their unique incompatibility to hydrophilic and hydrophobic segments. However, synthetic routes to heterograft copolymers consisting of a (semi)fluorinated backbone have not been developed yet.

Herein, synthesis of PCTFE-based heterograft copolymers containing aliphatic polyester and aromatic polymer side chains is presented. For the first time, a PCTFE graft copolymer containing polylactide (PLA) side chains is reported. Well-defined PLA-tethered VE (PLAVE) was synthesized by ring opening polymerization (ROP) of d,l-lactide, and then terpolymerized with CTFE and isobutyl vinyl ether (IBVE) to produce P(CTFE-*alt*-PLAVE)-*co*-P(CTFE-*alt*-IBVE). While CTFE and the VE monomers were alternately arranged in the backbone, grafting density of PLA side chains were controlled by adjusting the molar ratio between PLAVE and IBVE in the feed. The obtained graft copolymers were further utilized as ATRP macroinitiatiors for the grafting-from polymerization of styrene. Polystyrene (PS) side

chains grew from the CTFE repeating units in the backbone in a controlled manner, resulting in a heterograft copolymer bearing a hydrogenofluorinated backbone and both PLA and PS side chains. Microphase separation occurred in this heterograft copolymer driven by incompatibility of PLA to PS to produce a disordered morphology. We further demonstrate that controlled copolymerization of styrene with divinylbenzene produced cross-linked materials with the microphase-separated morphology generated *in situ* during the polymerization. Mesoporous polymers containing the fluorine-rich backbone on the pore surface can be obtained by selective removal of PLA. We believe that our methodology provides a synthetically more feasible route than the middle block approach, where the fluorinated polymer chain should be inserted between the sacrificial component and the matrix block of the block copolymer precursor. We note that such a porous polymer has not been reported to date, probably because multiblock copolymer synthesis including fluorinated polymer blocks is challenging. The heterograft architecture preorganizes the P(CTFE-*alt*-VE) backbone at the PLA/PS interface[22] that in turn becomes the pore surface after PLA removal, suggesting the usefulness of the synthetic route for tailoring pore surface.

Results and Discussion

A synthetic route to the heterograft copolymer containing PLA and PS side chains is depicted in Scheme 1. Graft-through polymerization of PLA was performed as a free radical terpolymerization of PLAVE, CTFE, and isobutyl vinyl ether (IBVE). The polymerization was carried out in an autoclave under pressure, initiated by bis(4-*tert*-butylcyclohexyl) peroxydicarbonate at 70 °C. Dimethyl carbonate (DMC) was used as a solvent to dissolve all reactants, which is considered a green organic solvent.[23] P(CTFE-*alt*-PLAVE)-*co*-P(CTFE-*alt*-IBVE) copolymers with controlled PLA molar mass and grafting density were successfully

produced. Then, ATRP of styrene (S) was performed at 100 °C in *N*-methyl-2-pyrrolidinone (NMP) in the presence of copper(I) bromide (CuBr) and 1,1,4,7,10,10-hexamethyltriethylenetetramine (HMTETA) following the previously reported procedure.[14]

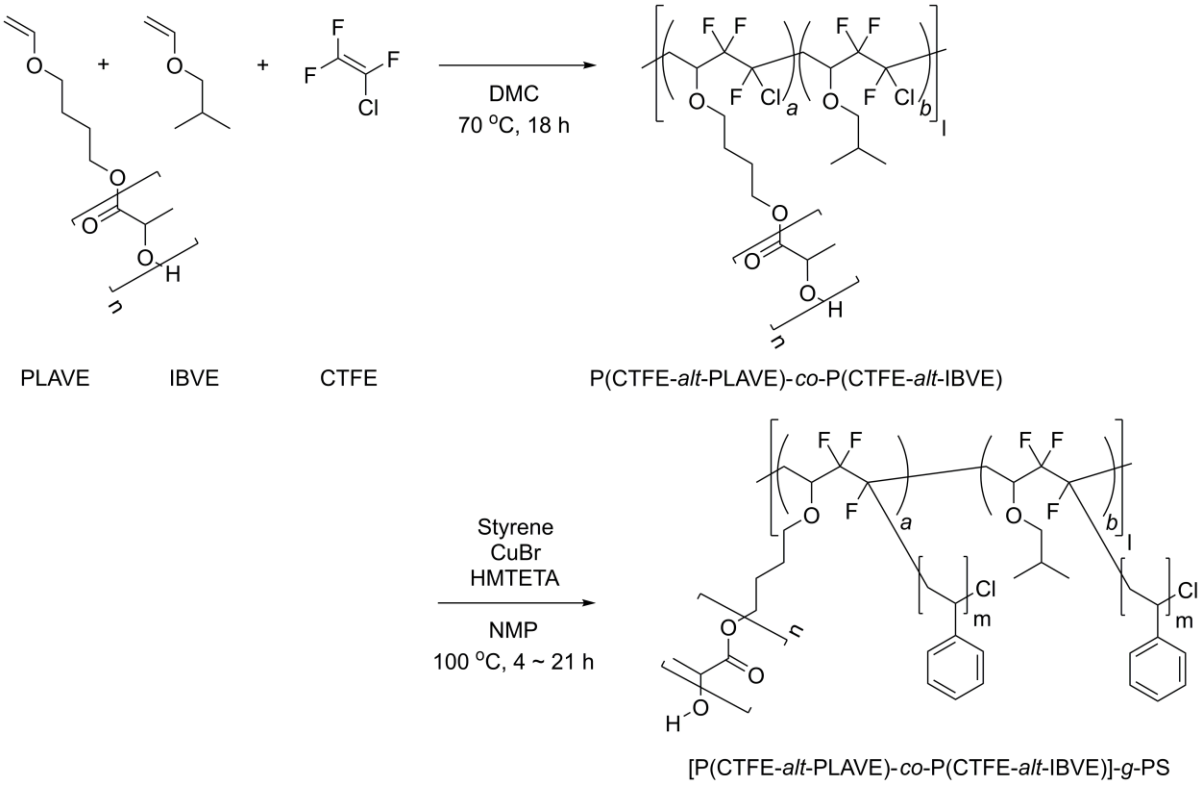

Scheme 1. Synthetic route to [P(CTFE-*alt*-PLAVE)-*co*-P(CTFE-*alt*-IBVE)]-*g*-PS graft copolymers

Grafting-through polymerization to PLA-grafted copolymer. Two PLAVEs with number-average molar mass (M_n) of 2 and 10 kg mol^{-1} were synthesized by ROP of d,l-lactide and used in this study. PLAVEs with dispersities ($Đ$) < 1.1 were produced by using 1,4-butanediol vinyl ether as an initiator and diazabicyclo[5,4,0]undec-7-ene (DBU) as a catalyst (Scheme S1 and Figure S1). ^{1}H nuclear magnetic resonance (NMR) spectra of PLAVEs obtained in deuterated dimethyl sulfoxide (DMSO-d_6) confirmed that the PLA macromonomers with a vinyl ether

terminus were successfully synthesized (Figure S2). $CDCl_3$ could not be used as a NMR solvent for the hydroxyl-functionalized vinyl ethers because of acetal formation via cyclization.[24-26]

Alternating copolymerization of CTFE and VE is typically performed in the presence of K_2CO_3 to avoid cationic polymerization of vinyl ether.[27] However, because PLA is susceptible to degradation in basic environments, the copolymerization was conducted without K_2CO_3. Molar ratio of CTFE to PLAVE+IBVE in the feed was set to 1:1 in all cases to facilitate an alternating behavior. Because of the strong electron-withdrawing character of CTFE, the alternating radical copolymerization proceeded well with the electron-rich vinyl ether even bearing a sterically bulky PLA pendent group. After the polymerization, we have not observed any VE monomer left from the ^{1}H NMR spectra of the crude product. The resulting copolymers were obtained as pale brown powders after 18 h of the terpolymerization and purified by precipitation in methanol twice. Higher loading of PLAVE or using higher molar mass PLAVE generally decreased the yield, presumably due to the steric hindrance in the polymerization.[28] The resulting copolymers were thoroughly analyzed by ^{1}H and ^{19}F NMR spectroscopies and size exclusion chromatography (SEC) as illustrated in Figure 1. In addition, their characterization details are summarized in Table 1. The graft copolymer is denoted as $PLA_n(x)$, where n and x represent degree of polymerization (DP) and grafting density of PLA, respectively.

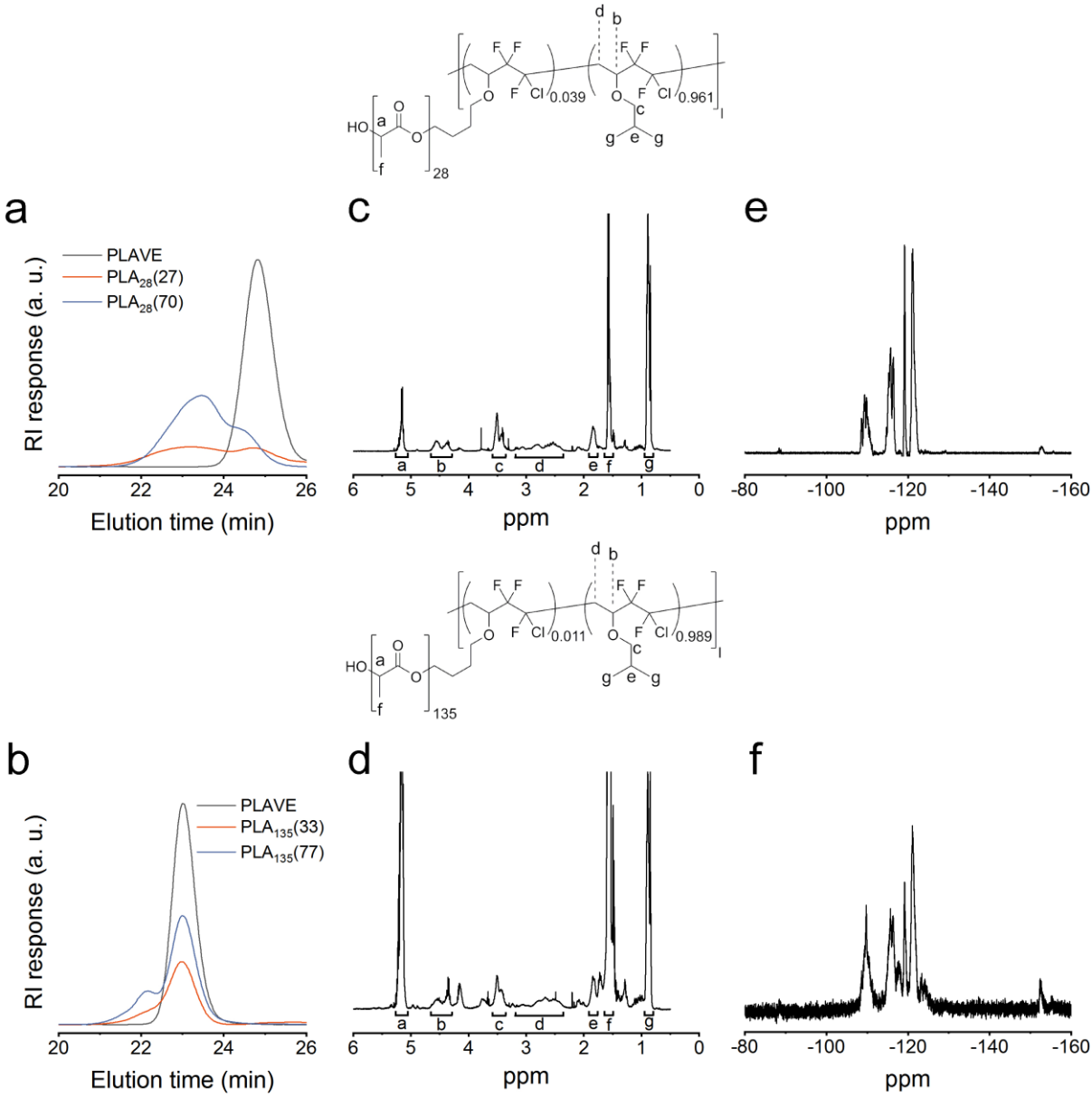

Figure 1. Characterization of P(CTFE-*alt*-PLAVE)-*co*-P(CTFE-*alt*-IBVE) (PLA$_n$(x)). (a-b) SEC traces of PLA$_{28}$(x)s (a) and PLA$_{135}$(x)s (b). (c-d) ^{1}H NMR spectra of PLA$_{28}$(27) (c) and PLA$_{135}$(33) (d). (e-f) ^{19}F NMR spectra of PLA$_{28}$(27) (e) and PLA$_{135}$(33) (f).

Table 1. Characterization of P(CTFE-*alt*-PLAVE)-*co*-P(CTFE-*alt*-IBVE) (PLA$_n$(x))

Sample	Feed ratio	Copolymer	M_n^c	M_w^c	$Đ^c$

				Composition[a,b]			(kg mol^{-1})	(kg mol^{-1})	
	PLAVE (mol%)	IBVE (mol%)	w_{PLA} (wt%)	PLAVE (mol%)	IBVE (mol%)	w_{PLA} (wt%)			
PLA_{28}(27)	4.0	96.0	27.1	3.9	96.1	26.9	16.6	23.3	1.40
PLA_{28}(70)	20.0	80.0	65.1	24.8	75.2	69.8	14.4	17.6	1.22
PLA_{135}(33)	0.8	99.2	26.4	1.1	98.9	32.8	20.4	24.2	1.19
PLA_{135}(77)	4.0	96.0	64.2	7.4	92.6	77.0	17.7	19.2	1.09

[a]PLAVE and IBVE molar fractions assessed by ^{1}H NMR spectroscopy (Equation S1)

[b]PLAVE weight fraction (w_{PLA}) assessed by ^{1}H NMR spectroscopy assuming that the copolymerization of VE and CTFE is perfectly alternating (Equation S2)

[c]Determined by chloroform-SEC based on linear PS calibration

For both PLAVEs, mixtures containing approximately 27 – 77 wt% of PLAVE were prepared and polymerized. When 2 kg mol^{-1} PLAVE was used, SEC traces of the resulting polymers showed a new peak corresponding to higher molar mass species, indicating a successful terpolymerization (Figure 1a). The PLAVE signal did not completely disappear in all cases. While this suggests incomplete consumption of PLAVE, we note that the signal by PLAVE appears more intense in the RI detector than that of the graft copolymer containing substantial amount of fluorine (PCTFE gives a negative signal because its refractive index (1.435) is smaller than that of chloroform (1.446)). Relatively increased signal intensity was observed indeed from the graft copolymers synthesized with higher PLAVE loading. ^{1}H NMR spectra in DMSO-d_6 indicated the absence of PLAVE vinyl protons in the product at least within the NMR resolution, supporting that most PLAVEs participated in the copolymerization (Figure S3). We note that even if a small amount of PLAVE may remain, the electron-rich vinyl

ether with such a sterically bulky pendent group should not participate in the copolymerization with styrene and thus should not affect the next grafting-from polymerization step.[29]

In addition to the peaks corresponding to protons originating from PLAVE and IBVE, a characteristic doublet of multiplets centered at 4.6 ppm evidences the presence of the methine group in the CTFE-$CH_2C\underline{H}$(OR)-CTFE triad (Figure 1c and 1d).[3, 5-7] This is in good agreement with an alternating copolymerization of CTFE with vinyl ethers. ^{19}F NMR spectra was also consistent with the graft copolymer structure, showing signals assigned to CF_2 and CFCl groups in the range of -123 to -108 ppm (Figure 1e and 1f).[27] A small signal at -154 ppm may correspond to CF_2H probably formed by chain transfer to solvent.[30] The graft copolymers synthesized with 10 kg mol^{-1} PLAVE displayed a similar trend but lower copolymerization efficiency than 2 kg mol^{-1} PLAVE, as evidenced by the SEC traces (Figure 1b).

Assuming a "perfect" alternating copolymerization, we estimated molar fractions of the repeating units by integrating ^1H NMR spectra of the graft copolymers (see Figure S4, Equations S1 – S2, and Table S1). The incorporation ratio was generally comparable to the feed composition, suggesting that the molar mass and grafting density of PLA side chain can be tuned.

Grafting-from polymerization to PLA/PS heterograft copolymers. ATRP was employed as the grafting-from polymerization technique to grow PS and produce PLA/PS heterograft copolymers. Polymerization kinetics was monitored using PLA_{28}(27) and PLA_{135}(33) as ATRP macroinitiators (see Figure 2, Table S2, Equations S3 – S5). Unless otherwise mentioned, an initial molar ratio of [-Cl]:[S]:[HMTETA]:[CuBr] = 1:20:0.08:0.08 was used following the literature condition.[14] The reaction mixture was diluted by NMP (390% of styrene volume), because the grafting-from polymerization is prone to termination between locally concentrated

radicals.[16,31,32] Conversion of styrene was monitored by checking the vinyl group consumption relative to NMP using ^{1}H NMR spectroscopy (see Figure S5, Equation S6 and Table S3). First-order kinetics showed an exponential decay of the styrene concentration over time (Figure 2a and b). Negative deviation from the linear relationship above 20 h was attributed to the termination reactions and the medium viscosity increase. The propagation rate was somewhat faster than the reported value for styrene grafting from PCTFE.[14]

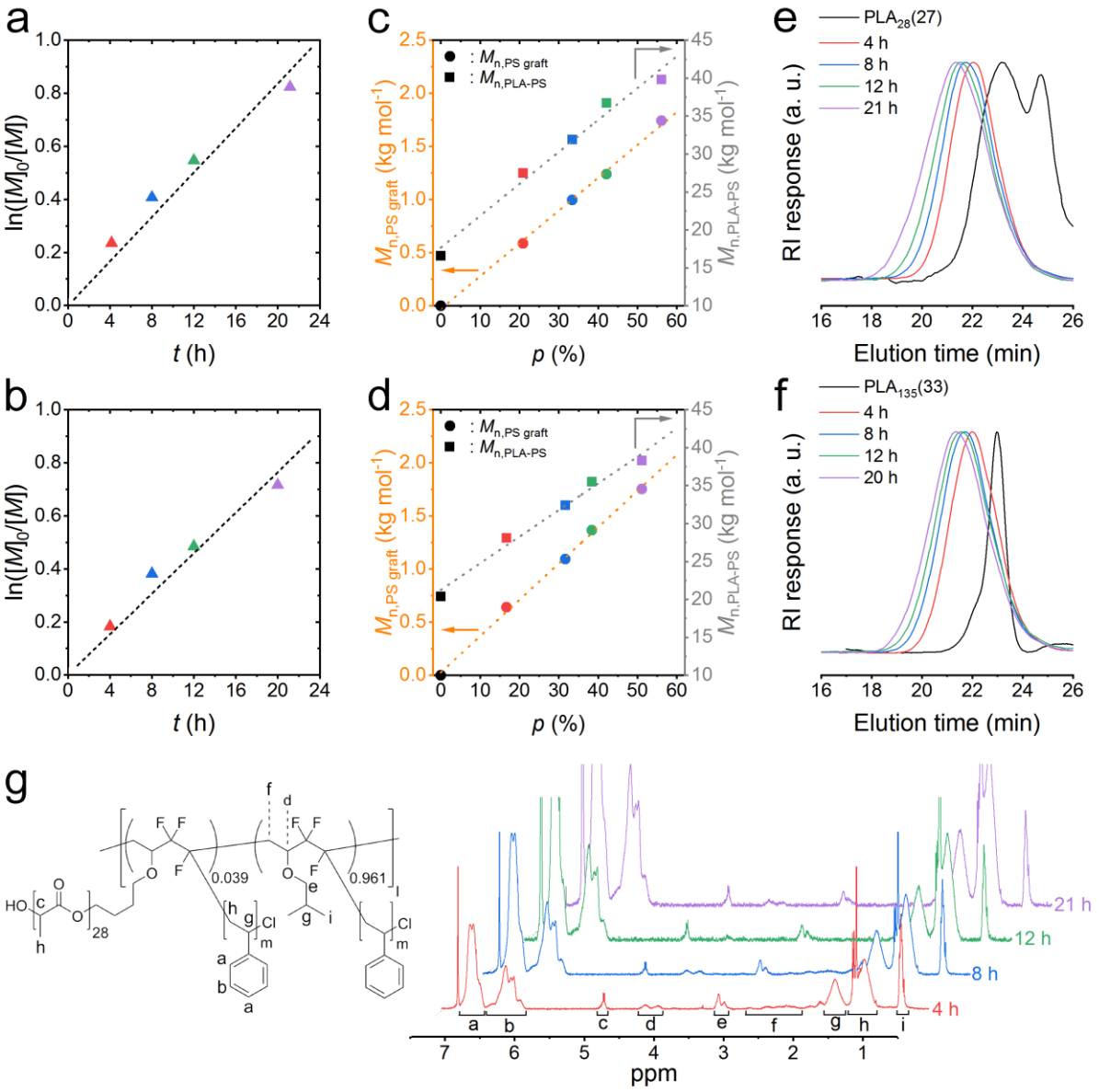

Figure 2. Grafting-from ATRP kinetics of styrene from $PLA_n(x)$ to produce [P(CTFE-*alt*-VE)-*g*-PLA-*co*-P(CTFE-*alt*-VE)]-*g*-PS graft copolymers. (a, c, e, g) Data obtained with $PLA_{28}(27)$. (b, d, f) Data obtained with $PLA_{135}(33)$. (a-b) First-order kinetic plots. (c-d) Conversion (p) vs. M_n plots. Dashed lines were obtained by linear regression of the data points. (e-f) Normalized SEC traces. (g) Stack of ^{1}H NMR spectra normalized by the signal intensity at 0.9 ppm.

SEC indicated that the whole molar mass ($M_{n,PLA-PS}$) increased linearly proportional to the conversion (p) (Figure 2c and d), also consistent to the controlled radical polymerization behavior. SEC traces also present a gradual shift as polymerization proceeded from 4 h to 20 - 21 h (Figure 2e and f). Tailing in the right-hand side was observed over time, however, presumably because dead chains would be formed by termination, resulting in the dispersity increase. In the ^{1}H NMR spectra of the heterograft copolymers, the integral ratio of the PLA methine proton centered at 5.2 ppm to the IBVE methyl proton at 0.9 ppm did not change much throughout the polymerization (Figure 2g). This suggests that PLA was intact in the employed ATRP condition. Signal intensity of PS aromatic protons at 6.3 – 7.3 ppm gradually increased with conversion. Molar mass of the PS side chain ($M_{n,PS}$) was estimated by integrating the signals with respect to the IBVE methyl proton (see Figure S6, Equation S7, and Table S3).

Under the established polymerization conditions, four PLA/PS heterograft copolymers with similar PS weight fractions (w_{PS}) (61 – 66%) were synthesized from different PLA graft copolymers for microphase separation studies (Figure S7 and Table S4). Table 2 summarizes their characterization data. The copolymers are denoted as $PLA_n(x)PS_m(y)$ following the notation of PLA graft copolymer, where n and m indicate their respective DPs while x and y represent the grafting densities.

Table 2. Characterization of [P(CTFE-*alt*-PLAVE)-*co*-P(CTFE-*alt*-IBVE)]-*g*-PS graft copolymers ($PLA_n(x)PS_m(y)$)

Sample	^{1}H NMR			SEC		
	w_{PLA}[a] (wt%)	$w_{P(CTFE\text{-}alt\text{-}VE)}$[a] (wt%)	w_{PS}[a] (wt%)	M_n[b] (kg mol^{-1})	M_w[b] (kg mol^{-1})	$Đ$[b]
$PLA_{28}(9)\,PS_5(66)$	9.2	25.2	65.6	23.0	50.8	2.21
$PLA_{28}(27)PS_{11}(61)$	27.1	11.8	61.1	24.7	47.0	1.90
$PLA_{135}(11)PS_6(66)$	11.2	23.0	65.8	17.1	34.4	2.02
$PLA_{135}(24)PS_{19}(65)$	24.2	10.4	65.4	36.3	136.5	3.75

[a]Weight fraction of PLA graft, P(CTFE-*alt*-VE) backbone, and PS graft (Equations S3 – S5)

[b]Determined by chloroform-SEC based on linear PS calibration

Differential scanning calorimetry (DSC) analysis of the heterograft copolymers showed two glass transition temperatures (T_gs) at 40 – 48 and 88 – 96 °C (Figure S8). These were assigned to T_gs of PLA and PS, suggesting the side chains are segregated via microphase separation. While glass transition of P(CTFE-*alt*-IBVE) is known to be observed at 23 °C,[33] we have not observed other thermal transitions in the range of -80 to 200 °C. We also note that T_g of P(CTFE-*alt*-IBVE) was not observed from the thermograms of $PLA_n(x)$s either (Figure S9).

Figure 3a presents the small angle X-ray scattering (SAXS) data of the heterograft copolymers. A broad scattering peak was generally observed, and its scattering intensity was significantly increased with increasing PS molar mass. Domain spacing (d) was estimated from

the peak position (q^*) by following relationship $d = 2\pi/q^*$. A slight increase in d from 19 to 21 nm was observed by increasing DP of PLA from 28 to 135, but the length scale substantially increased with the increasing DP of PS. This suggests that microphase separation is mainly driven by incompatibility of PLA to PS, and the segregation strength increases with the increasing PS molar mass. The low degree of order appears to stem from the complex and highly asymmetric graft architecture. Only a few but much longer PLA side chains would be scattered over the backbone, whereas very short PS chains would be grafted per every two repeating units in an ideal scenario.

A transmission electron microscopy (TEM) image of $PLA_{28}PS_{11}$ also supports the formation of a disordered morphology (Figure 3b). Dark and light areas were assigned to PS and PLA microdomains, respectively, based on the previous study.[34,35] The P(CTFE-*alt*-VE) backbone should be located at the interface, but it was not discernable due to lack of contrast. Interdomain distance was comparable to the d values obtained from the SAXS data.

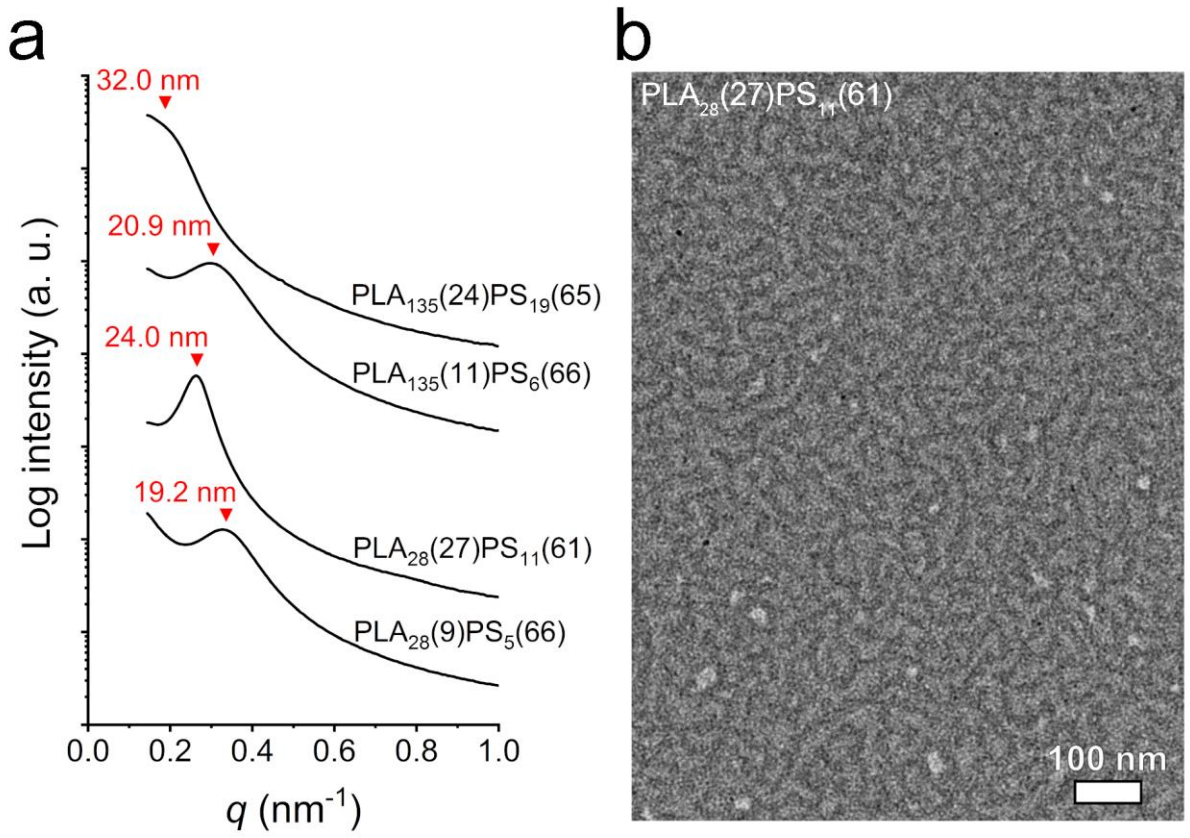

Figure 3. (a) SAXS data of PLA$_n$(x)PS$_m$(y)s. (b) Representative TEM image of PLA$_{28}$(27)PS$_{11}$(61).

Grafting-from copolymerization of S and DVB for the synthesis of mesoporous polymers. Growth of the second polymer chain in the presence of the highly incompatible first polymer offers an opportunity to apply the polymerization-induced microphase separation (PIMS) on the graft architecture. We hypothesized that the copolymerization of styrene and divinylbenzene (DVB) in ATRP process would produce a cross-linked P(S-*co*-DVB) domain *in situ* and spontaneously segregates PLA, as reported in the reversible addition-fragmentation chain transfer (RAFT) copolymerization of styrene and DVB in the presence of PLA macro-chain transfer agent.[36,37] PLA etching would produce a robust porous polymer where the

densely cross-linked P(S-*co*-DVB) framework firmly supports the nanopore structure. Since the P(CTFE-*alt*-VE) backbone would be located between PLA and PS, fluorine-rich pore surface may be obtained and useful for antifouling and improving chemical stability.[38,39] It is noteworthy that introducing fluorinated polymers as a middle block between PLA and PS may be also considered for tailoring the pore surface.[40] Controlling the microphase separation process from a homogeneous polymerization mixture, however, may be more challenging because of strong incompatibility of fluorinated polymers with hydrocarbon polymers.

The copolymerization of S and DVB in bulk was attempted by using PLA_{28}(70) or PLA_{135}(77) as macroinitiators, where the grafting density of PLA is high. The PLA weight fraction in the product was targeted as approximately 27 – 30 wt%. The [S]:[DVB] molar ratio was varied from 90:10 to 0:100 to investigate the effect of the cross-linking density. Solvent was not included in the polymerization mixture to increase the segregation strength between PLA and PS. Monolithic copolymers with >90% yield were successfully obtained in most cases after 20 h of polymerization at 100 °C (Table S5). Lower yields (74 – 85%) were observed with PLA_{28}(70) at low DVB loading. SAXS data of the polymers exhibited a broader scattering peak compared to PLA/PS heterograft copolymers. The peak became more diffuse with the increasing DVB content (Figures S10 and S11). This is consistent with the PIMS scheme of arresting the emerging disordered bicontinuous morphology of PLA and P(S-*co*-DVB) by *in situ* cross-linking.[41] The cross-linking onset is strongly influenced by the DVB content.[42] Higher DVB loading leads the morphology to be captured in a more disordered state as noted by broadening of the scattering peak, because of decreased mobility by the accelerated cross-linking in the early stage of polymerization. However, compared to the conventional PIMS process, the peak width is noticeably large reflecting substantial heterogeneity induced by the heterograft architecture. The length scale of microphase separation seems to be primarily

determined by the PLA molar mass. In case of samples synthesized with $PLA_{135}(77)$, the q^* position was not discernable due to the large length scale.

PLA was selectively degraded by treating with NaOH solution to create the corresponding void percolating the cross-linked P(S-*co*-DVB) matrix. Generally, weight loss by the basic treatment was in agreement with the PLA weight fraction in the precursor (Table S5). Removal of PLA was confirmed by FTIR spectroscopy showing the vanishing of C=O stretching of PLA at 1745 cm^{-1} highlighted in Figure S12. SAXS data after PLA etching showed significantly increased scattering intensities because of much higher electronic density contrast between the void and the remaining polymer. Shape of the scattering patterns was reminiscent of the parents suggesting formation of pores templated by the PLA domains. Capillary condensation at high relative pressure is apparently noticed in the nitrogen sorption isotherms displayed in Figure 4a and b, clearly supporting the presence of mesopores. Specific surface area (S_{BET}) was calculated by Brunauer-Emmett-Teller analysis.[43] By Barrett-Joyner-Halenda (BJH) analysis[44] of the desorption branch, mean pore size (D_{BJH}) was estimated to be 3.7 – 4.3 nm and 6.4 – 10.4 nm templated by $PLA_{28}(70)$ and $PLA_{135}(77)$ with different DVB contents (Figure S13). This supports that the pore size is primarily governed by the PLA molar mass.[41] A slight decrease in pore size with the increasing DVB fraction was also consistent with the literature.[42] At the high DVB fraction, densely cross-linked microgels are thought to be formed by S/DVB copolymerization, and further aggregated and loosely bridged to produce macrogelation. Because of the bulky nature of microgels, the PLA chain density is reduced at the interface leading to chain contraction to fill the space. This leads to the slight decrease in the pore size with increasing DVB content. In case of $PLA_{135}(77)$, porosity of 0.31 – 0.38 mL g^{-1} was consistently observed regardless of DVB fraction and in good agreement with the initial PLA content in the polymerization mixture.[41] For $PLA_{28}(70)$, however, low DVB loading

seems to be insufficient for stabilizing the small pores and to induce partial pore collapse, indicated by lower porosity.[45] Their pore characteristics are summarized in Table 3. Scanning electron microscopy (SEM) images also support that 3D continuous mesopores are well developed throughout the specimen (Figure 4c and d). Energy-dispersive X-ray spectroscopy (EDS) data indicate the presence of fluorine in all mesoporous polymers, suggesting that the mesopore surface would be decorated with fluorine atoms (Figure S14).

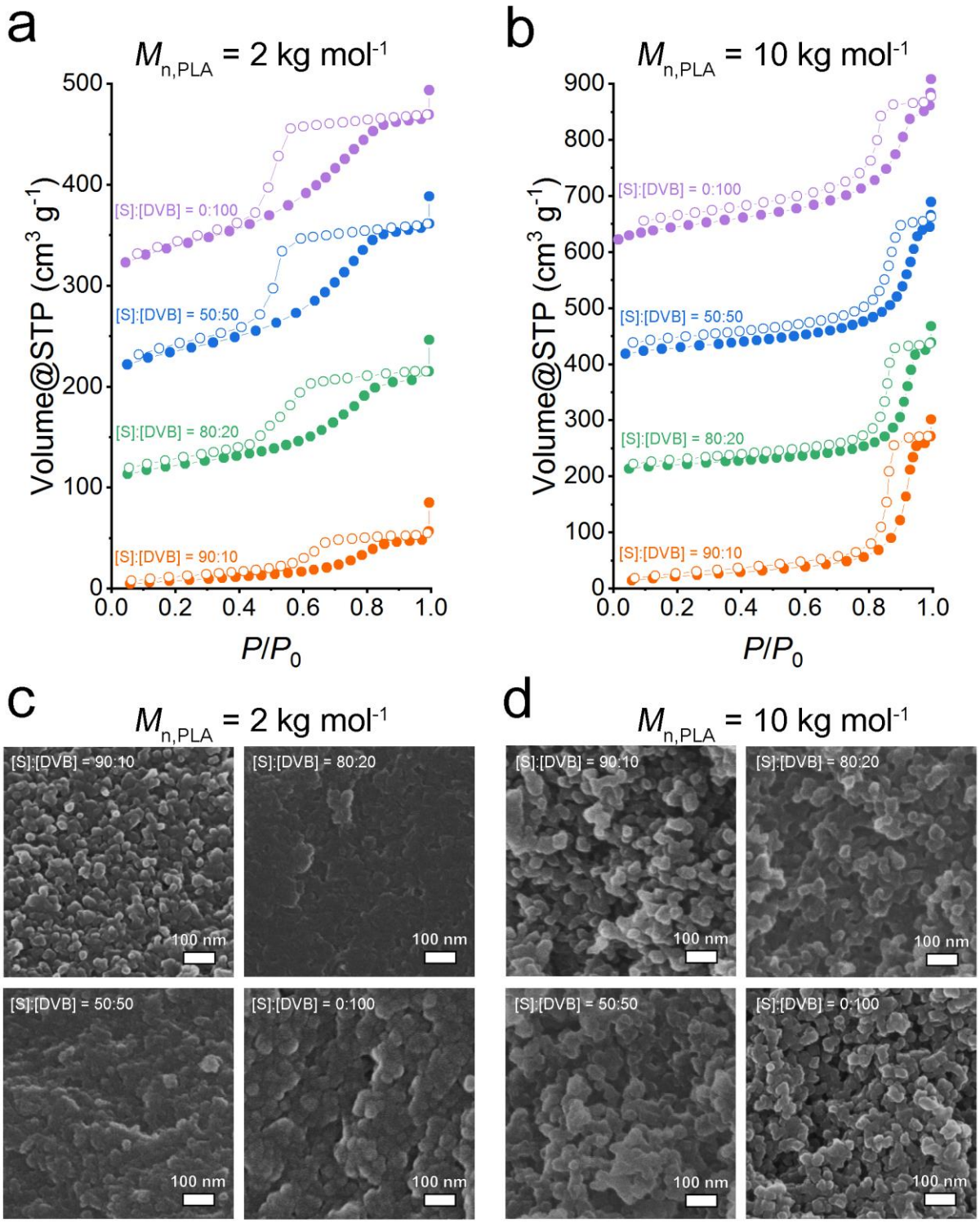

Figure 4. Characterization of mesoporous polymers derived from [P(CTFE-*alt*-PLAVE)-*co*-P(CTFE-*alt*-IBVE)]-*g*-P(S-*co*-DVB) graft copolymers. (a, b) Nitrogen sorption isotherms. (c, d) SEM images.

Table 3. Pore characteristics of mesoporous copolymers derived from [P(CTFE-*alt*-PLAVE)-*co*-P(CTFE-*alt*-IBVE)]-*g*-P(S-*co*-DVB) graft copolymers

Macroinitiator	[S]:[DVB]	S_{BET}[a] ($m^2\ g^{-1}$)	V_{total}[b] ($cm^3\ g^{-1}$)	D_{BJH}[c] (nm)
PLA_{28}(70)	0:100	154	0.23	3.7
	50:50	139	0.21	3.8
	80:20	85	0.15	3.8
	90:10	30	0.07	4.3
PLA_{135}(77)	0:100	169	0.36	6.4
	50:50	112	0.35	8.2
	80:20	77	0.31	9.6
	90:10	80	0.38	10.4

[a]Specific surface area calculated from $0.05 < P/P_0 < 0.20$ by BET analysis

[b]Total pore volume calculated from the point near $P/P_0 = 0.95$

[c]Mean pore size calculated by BJH method

In conclusion, unprecedented heterograft copolymers with fluorinated backbone were successfully synthesized. The first graft, PLA, was attached on the backbone by "grafting-through" approach. Straightforward radical copolymerization of PLAVE and CTFE could afford PLA-grafted fluoropolymer, where PLA size and grafting density could be controlled. Then "grafting-from" approach was employed to attach PS grafts on the backbone *via* ATRP from the chlorine atoms of CTFE units. The size of PS grafts could be varied by changing the reaction time. The microphase separation between PLA and PS was confirmed by SAXS and

TEM, which also supports that PLA and PS were covalently bonded to the backbone. Furthermore, these graft copolymers were utilized as templates to induce mesoporous structure. Cross-linking via ATRP copolymerization of S and DVB from PLA_{28}(70) and PLA_{135}(77) followed by PLA etching yields 4 and 10 nm-sized pores within bicontinuous structures. Considering the straightforward incorporation of PLA and PS grafts onto a semifluorinated backbone and the pore size-controllability, such a novel synthetic route to produce heterograft copolymers and their uses for mesoporous structures holds a potential use toward future applications (e.g. water treatment) where fluorinated pore surface is highly demanding.

Experimental Section

Materials. Chlorotrifluoroethylene (CTFE) was kindly provided from Honeywell (Moristown, USA). Bis(4-*tert*-butylcyclohexyl) peroxydicarbonate was purchased from AkzoNobel (Amsterdam, Netherlands). Both d-lactide (99%) and l-lactide (99%) were kindly provided by Corbion Purac (Amsterdam, Netherlands). d,l-Lactide was obtained from recrystallizing the same amount of d-lactide and l-lactide in ethyl acetate. Dimethyl carbonate (DMC) (>99%), 1,4-butanediol vinyl ether (99%), diaza-bicyclo[5,4,0]undec-7-ene (DBU) (≥99%), isobutyl vinyl ether (IBVE) (99%), styrene (S) (99.9%), divinylbenzene (DVB) (80%, tech.), copper(I) bromide (CuBr) (99.999%), 1,1,4,7,10,10-hexamethyltriethylenetetramine (HMTETA) (97%), and *N*-methyl-2-pyrrolidone (NMP) (anhydrous, 99.5%) were purchased from Sigma-Aldrich (St. Louis, MO). S and DVB were used after the removal of inhibitor by filtering through basic aluminum oxide column. The other chemicals were used as received. HPLC grade dichloromethane (DCM) was purchased from J. T. Baker (Center Valley, PA). Benzoic acid (99.5%), sodium hydroxide (>97%), and other laboratory chemicals used in

work-up process were purchased from Daejung (Siheung, Korea). Epoxy resin and hardener (KEM90) were purchased from ATM GmbH (Mammelzen, Germany).

Methods. For the characterization of polylactide-tethered vinyl ether (PLAVE) and P(CTFE-*alt*-PLAVE)-*co*-P(CTFE-*alt*-IBVE) copolymer, ^{1}H and ^{19}F nuclear magnetic resonance (NMR) spectra were recorded on a Bruker AC 400 Spectrometer (400 MHz for ^{1}H and 376 MHz for ^{19}F NMR) using $CDCl_3$ and dimethyl sulfoxide-d_6 as solvent. The sample temperature was set to 298 K. Chemical shifts and coupling constants are given in Hertz (Hz) and parts per million (ppm), respectively. The experimental conditions for recording the ^{1}H and ^{19}F NMR spectra were as follows. For ^{1}H NMR spectra, flip angle, acquisition time, pulse delay, and the number of scans were 90°, 4.5 s, 2 s, and 32 respectively. For ^{19}F NMR spectra, they were 30°, 0.7 s, 5 s, and 64 respectively with a pulse width of 5 μs. For the characterization of [P(CTFE-*alt*-PLAVE)-*co*-P(CTFE-*alt*-IBVE)]-*g*-PS, ^{1}H NMR spectroscopy was conducted using a Bruker Avance 400 MHz spectrometer (Billerica, MA) using the residual NMR solvent signal as an internal reference. The molar mass and dispersity ($Đ$) of PLAVE were measured using an Agilent Infinity 1260 series (Santa Clara, CA) size exclusion chromatography (SEC) system equipped with an Optilab UT-rEX refractive index detector (Santa Barbara, CA) and PLgel 10 mm MIXED-B columns. Chloroform was used as an eluent at 35 °C, and the number- and weight-average molar masses ($M_{n,SEC}$ and $M_{w,SEC}$) of the polymers were calculated relative to linear polystyrene standards (EasiCal) purchased from Agilent Technologies. Fourier transform infrared (FTIR) spectra were obtained on a Bruker Alpha FTIR spectrometer using a Platinum ATR (attenuation total reflection) single reflection module. Differential scanning calorimetry (DSC) study was conducted on Netzsch DSC 204 F1 Phoenix (Selb, Germany) using a scan rate of 10 °C/min under N_2 atmosphere. The thermogram from the second heating

was used to assess T_g. Synchrotron small-angle X-ray scattering (SAXS) experiments were performed at 9A U-SAXS beam line in Pohang Accelerator Laboratory (PAL). A monochromatized X-ray radiation source of 11.025 keV with the sample-to-detector distance of 4.437 m was used. Scattering intensity was monitored by a Mar 165 mm diameter CCD detector with 2048×2048 pixels. The two-dimensional scattering patterns were azimuthally integrated to afford one-dimensional profiles presented as scattering vector (q) versus scattering intensity, where the magnitude of scattering vector is given by $q = (4\pi/\lambda)\sin\theta$. The samples were annealed at 110 °C for 12 h prior to SAXS experiments. Scanning electron microscope (SEM) images were obtained on a Hitachi S-4700 FE-SEM (Schaumbur, IL) with a 5 kV accelerating voltage and an upper secondary electron detector. Samples were coated with OsO_4 prior to imaging. Energy-dispersive X-ray spectroscopy (EDS) analysis was conducted using FEI Magellan 400 FE-SEM after coating with OsO_4. Transmission electron microscopy (TEM) was performed on a Jeol JEM-2100F field-emission transmission electron microscope (Tokyo, Japaan) with acceleration voltage of 200 kV. Annealed samples at 100 °C were embedded in epoxy (KEM90) and cured. The hardened samples were sectioned to below 100 nm thickness using a RMC Boeckeler PTPC PowerTome Ultramicrotome (Tucson, AZ) equipped with a diamond knife. They were transferred onto 300 mesh carbon-coated copper grids and stained with RuO_4 prior to imaging. Nitrogen sorption isotherms were obtained on a Mirae SI nanoPOROSITY-XQ analyzer (Gwangju, Korea) at the temperature of liquid nitrogen (77.3 K). Mode pore diameter (D_{N2}) was estimated by Barrett-Joyner-Halenda (BJH) analysis of the desorption branch of nitrogen sorption isotherms.[44]

Synthesis of PLAVE. Polylactide-tethered vinyl ether (PLAVE) was synthesized by ring-opening transesterification polymerization (ROTEP) of d,l-lactide in the presence of

hydroxyl 1,4-butanediol vinyl ether as an initiator and DBU as a catalyst (Scheme S1). Synthesis of 10 kg mol^{-1} PLAVE is given here as an example. In a glove box, 1,4-butandiol vinyl ether (0.20 g, 1.73 mmol) and d,l-lactide (25.00 g, 173.44 mmol) were placed in a pressure vessel and dissolved in DCM (250 mL). Polymerization was initiated by adding DBU (131 μL, 0.88 mmol) to the mixture. After stirring the mixture for 25 min at R.T, the polymerization was quenched by adding benzoic acid (0.33 g, 2.78 mmol). The polymerization mixture was precipitated from methanol and PLAVE was obtained by filtration. The PLAVE was further purified by reprecipitation in *n*-hexane and dried in vacuum at 40 °C overnight (16.69 g, 67%). For the synthesis of 2 kg mol^{-1} PLAVE, the amount of 1,4-butanediol vinyl ether was increased to 1.34 g (11.56 mmol) as 1/15 equivalent to d,l-lactide. The crude product was precipitated in cold methanol (-20 °C) followed by drying overnight at R.T. (18.18 g, 73%).

The number-average molar masses of PLAVEs (M_n) were assessed by NMR spectroscopy taking into account the integrals of the methine peak centered at 5.2 ppm with respect to those of the vinyl protons. The M_n values were 2 and 10 kg mol^{-1} when [d,l-lactide]:[1,4-butanediol vinyl ether] ratios were 15:1 and 100:1 in the feed, respectively. Based on SEC analyses, their M_ns (and dispersities) were 3.8 (1.09) and 17.6 kg mol^{-1} (1.06), respectively.

Synthesis of P(CTFE-*alt*-PLAVE)-*co*-P(CTFE-*alt*-IBVE) (PLA$_n$(*x*)). Synthesis of PLA_{28}(27) (Table S1) is given here as an example based on the previously reported procedure.[27,46] The terpolymerization of PLAVE, IBVE, and CTFE was carried out in a 50-mL Hastelloy autoclave Parr system (HC 276) equipped with a manometer, a mechanical Hastelloy anchor, a rupture disk (3000 PSI), inlet and outlet valves equipped with a special steel pipe, and a Parr electronic controller for stirring speed and heating control. Initially, the autoclave was closed and put under vacuum (10^{-2} mbar) in order to remove any residual traces of oxygen.

Then, a degassed solution composed of bis(4-*tert*-butylcyclohexyl) peroxydicarbonate (1.37 g, 3.43 mmol), PLAVE (7.27 g, 3.43 mmol), IBVE (8.26 g, 82.43 mmol), and DMC (30 mL) was transferred through a funnel tightly connected to the inlet valve of the autoclave. The reactor was then cooled in a liquid nitrogen bath, and CTFE gas (10 g, 85.86 mmol) was introduced under weight control. Subsequently, the autoclave was warmed up to R.T. and gradually heated to 70 °C while the reaction solution was mechanically stirred. The copolymerization was conducted at that temperature for 18 h. Then, the vessel was cooled to R.T. and immersed in an ice bath for 30 min. Finally, after depressurization by venting unreacted CTFE off, the autoclave was opened. The purified product was obtained after two repeated precipitations from a 10-fold excess (400 mL) of methanol, followed by drying under vacuum at 40 °C overnight. The final product was recovered as pale brown powder (20.46 g, 80 %) and characterized by ^{1}H and ^{19}F NMR spectroscopy and SEC. PLA_{28}(70) (23.41 g, 44%), PLA_{135}(33) (15.29 g, 60%), and PLA_{135}(77) (31.27 g, 59%) were obtained by following the same procedure but with different [PLAVE]:[IBVE] molar ratios.

Synthesis of [P(CTFE-*alt*-PLAVE)-*co*-P(CTFE-*alt*-IBVE)]-*g*-PS graft copolymers (PLA_n(*x*)PS_m(*y*)). ATRP of styrene was performed based on the protocols reported in the literature.[14] Synthesis of PLA_{28}(9)PS_5(66) in Table S4 is given here as an example. A solution of PLA_{28}(27) (0.3 g, 1.016 mmol of Cl), styrene (2.10 g, 20.18 mmol), HMTETA (0.019 g, 0.08 mmol), and CuBr (0.012 g, 0.08 mmol) was prepared in NMP (9.0 mL, 390% of styrene volume) and placed in an ampule equipped with a stirring bar. The molar ratio of [-Cl]:[S]:[HMTETA]:[CuBr] = 1:20:0.08:0.08 was targeted. The mixture was degassed by three cycles of freeze-pump-thaw and then put in the oil bath preset at 100 °C for 16 h. After cooling to R.T., the resulting polymer was recovered by precipitation from methanol, and dried in vacuum at 40 °C for overnight (0.67 g, 28%).

The total number of Cl in 0.3 g of $PLA_n(x)$ is calculated by assuming 100% alternating behavior as follows:

$$\frac{\#\ \text{of Cl}}{0.3\ \text{g of PLA}_n(x)} = \frac{0.3 \times 100}{(a \times (DP_{\text{PLA}} \times 72.07 + M_{\text{VE+CTFE}}) + b \times M_{\text{IBVE+CTFE}})}$$

where *a*, and *b* represent the molar fraction of PLAVE and IBVE, respectively and $M_{\text{VE+CTFE}}$ and $M_{\text{IBVE+CTFE}}$ denote molar mass sums of the indicated repeating units (all of the values are available in Equation S2 and Table S1).

Following the protocol described above, the other $PLA_n(x)PS_m(y)$s were synthesized by varying the reaction time. In case of $PLA_{135}(24)PS_{19}(65)$, the molar ratio of [-Cl]:[S]:[HMTETA]:[CuBr] = 1:30:0.13:0.13 was used. The conversion and yield of $PLA_n(x)PS_m(y)$s are listed in Tables S2 and S4 accordingly.

Synthesis of [P(CTFE-*alt*-PLAVE)-*co*-P(CTFE-*alt*-IBVE)]-*g*-P(S-*co*-DVB) graft copolymer and derivation of mesoporous polymer. Synthesis of [P(CTFE-*alt*-PLAVE)-*co*-P(CTFE-*alt*-IBVE)]-*g*-P(S-*co*-DVB) graft copolymer from $PLA_{28}(70)$ with S:DVB = 1:1 molar ratio is given here as an example. A solution of $PLA_{28}(70)$ (0.45 g, 0.628 mmol of Cl), styrene (0.31 g, 2.99 mmol), DVB (0.39 g, 2.99 mmol), HMTETA (0.034 g, 0.15 mmol), and CuBr (0.021 g, 0.15 mmol) was placed in an ampule equipped with a stirring bar. The molar ratio of [-Cl]:[HMTETA]:[CuBr] = 1:0.25:0.25 was targeted, and the weight fraction of $PLA_{28}(70)$ in the polymerization mixture was set to 39%. The mixture was degassed by three cycles of freeze-pump-thaw and then placed in the oil bath preset at 100 °C for 20 h. After cooling to R.T, the monolithic solid was recovered by crushing the ampule and dried in the ambient condition to remove unreacted monomers (1.18 g, 97%). The other [P(CTFE-*alt*-PLAVE)-*co*-P(CTFE-*alt*-IBVE)]-*g*-P(S-*co*-DVB) graft copolymers from $PLA_{135}(77)$ were synthesized by varying the S:DVB molar ratio while [-Cl]:[HMTETA]:[CuBr] ratio is

1:0.33:0.33 and the weight fraction of PLA_{135}(77) is 39%.

PLA was etched out of the cross-linked precursor following the literature protocol.[41] The cross-linked precursor, [P(CTFE-*alt*-PLAVE)-*co*-P(CTFE-*alt*-IBVE)]-*g*-P(S-*co*-DVB) was placed within a polypropylene vial filled with 0.5 M NaOH solution (methanol/water = 4/6 (v/v)). The vial was sealed with electrical tape and heated in an oil bath at 70 °C for 3 days. The mesoporous monolith was obtained by draining the solution and thoroughly rinsed with water and methanol iteratively. The monolith was dried in vacuum at R.T for overnight. The precursor and resulting mesoporous polymer yields are listed in Table S5.

Acknowledgements

This research was supported by the International Research & Development Program the National Research Foundation of Korea (NRF) funded by the Ministry of Science and ICT (2018K1A3A1A21043905). The authors also thank the STAR-Programme Hubert Currien bilateral project. Experiments at Pohang Accelerator Laboratory (PAL) were supported in part by Ministry of Science and ICT of Korea and POSTECH. TEM imaging was conducted in Korea National NanoFab Center supported by Nano Material Technology Development Program through the National Research Foundation of Korea (NRF) funded by the Ministry of Science and ICT (2009-0082580). Corbion Purac (Amsterdam, Netherlands) and Honeywell Company (Morristown, USA) are acknowledged for providing free samples of lactide and CTFE, respectively.

Associated Content: Synthetic scheme and SEC traces of PLAVEs, ^{1}H NMR spectra of 1,4-butanediol vinyl ether, PLAVEs, and $PLA_n(x)$s, ^{1}H NMR, SEC, and DSC data of $PLA_n(x)PS_m(y)$, SAXS and FTIR data of cross-linked precursors and the resulting mesoporous

polymers, BJH pore size distribution and EDS data of the mesoporous polymers, description on calculation details of weight fractions, ATRP conversions, DPs and molar masses of PS.

References

1. Boschet, F.; Améduri, B. (Co)polymers of Chlorotrifluoroethylene: Synthesis, Properties, and Applications. *Chem. Rev.* **2014,** *114*, 927-980.

2. Boutevin, B.; Cersosimo, F.; Youssef, B. Studies of the Alternating Copolymerization of Vinyl Ethers with Chlorotrifluoroethylene. *Macromolecules* **1992,** *25*, 2842-2846.

3. Carnevale, D.; Wormald, P.; Améduri, B.; Tayouo, R.; Ashbrook, S. E. Multinuclear Magnetic Resonance and DFT Studies of the Poly(chlorotrifluoroethylene-*alt*-ethyl vinyl ether) Copolymers. *Macromolecules* **2009,** *42*, 5652-5659.

4. Hoshino, T.; Morizawa, Y. Fluorinated Specialty Chemicals – Fluorinated Copolymers for Paints and Perfluoropolyethers for Coatings. In *Fluorinated Polymers: Volume 2: Applications*; Améduri, B.; Sawada, H., Eds.; The Royal Society of Chemistry: London, 2017; pp 110-126.

5. Alaaeddine, A.; Couture, G.; Améduri, B. An Efficient Method to Synthesize Vinyl Ethers (VEs) that Bear Various Halogenated or Functional Groups and Their Radical Copolymerization with Chlorotrifluoroethylene (CTFE) to Yield Functional Poly(VE-*alt*-CTFE) Alternated Copolymers. *Polym. Chem.* **2013,** *4*, 4335-4347.

6. Alaaeddine, A.; Boschet, F.; Améduri, B.; Boutevin, B. Synthesis and Characterization of Original Alternated Fluorinated Copolymers Bearing Glycidyl Carbonate Side Groups. *J. Polym. Sci., Part A: Polym. Chem.* **2012,** *50*, 3303-3312.

7. Campagne, B.; David, G.; Améduri, B.; Jones, D. J.; Rozière, J.; Roche, I. Novel Blend Membranes of Partially Fluorinated Copolymers Bearing Azole Functions with Sulfonated PEEK for PEMFC Operating at Low Relative Humidity: Influence of the Nature of the *N*-Heterocycle. *Macromolecules* **2013,** *46*, 3046-3057.

8. Frutsaert, G.; Delon, L.; David, G.; Améduri, B.; Jones, D. J.; Glipa, X.; Rozière, J.

Synthesis and Properties of New Fluorinated Polymers Bearing Pendant Imidazole Groups for Fuel Cell Membranes Operating over a Broad Relative Humidity Range. *J. Polym. Sci., Part A: Polym. Chem.* **2010,** *48*, 223-231.

9. Tillet, G.; De Leonardis, P.; Alaaeddine, A.; Umeda, M.; Mori, S.; Shibata, N.; Aly, S. M.; Fortin, D.; Harvey, P. D.; Améduri, B. Design and Photonic Properties of Novel Fluorinated Copolymers Bearing Phthalocyanine Side Groups. *Macromol. Chem. Phys.* **2012,** *213*, 1559-1568.

10. Alaaeddine, A.; Hess, A.; Boschet, F.; Allcock, H.; Améduri, B. Synthesis and Characterization of Novel Alternating Fluorinated Copolymers Bearing Oligo(ethylene oxide) Side Chains. *J. Polym. Sci., Part A: Polym. Chem.* **2013,** *51*, 977-986.

11. Taylor, R. T.; Shah, J. A.; Green, J. W.; Kamolratanayothin, T. Poly(Chlorotrifluoroethylene) Substitution Reactions. In *Polymer Modification*; Swift, G.; Carraher, C. E.; Bowman, C. N., Eds.; Springer US: Boston, MA, 1997; pp 133-151.

12. Tsang, E. M. W.; Zhang, Z.; Shi, Z.; Soboleva, T.; Holdcroft, S. Considerations of Macromolecular Structure in the Design of Proton Conducting Polymer Membranes: Graft versus Diblock Polyelectrolytes. *J. Am. Chem. Soc.* **2007,** *129*, 15106-15107.

13. Yang, A. C. C.; Narimani, R.; Zhang, Z.; Frisken, B. J.; Holdcroft, S. Controlling Crystallinity in Graft Ionomers, and Its Effect on Morphology, Water Sorption, and Proton Conductivity of Graft Ionomer Membranes. *Chem. Mater.* **2013,** *25*, 1935-1946.

14. Valade, D.; Boschet, F.; Améduri, B. Grafting Polymerization of Styrene onto Alternating Terpolymers Based on Chlorotrifluoroethylene, Hexafluoropropylene, and Vinyl ethers, and Their Modification into Ionomers Bearing Ammonium Side-Groups. *J. Polym. Sci., Part A: Polym. Chem.* **2010,** *48*, 5801-5811.

15. Tan, S.; Li, J.; Zhang, Z. Study of Chain Transfer Reaction to Solvents in the Initiation

Stage of Atom Transfer Radical Polymerization. *Macromolecules* **2011,** *44*, 7911-7916.

16. Zhang, M.; Russell, T. P. Graft Copolymers from Poly(vinylidene fluoride-*co*-chlorotrifluoroethylene) via Atom Transfer Radical Polymerization. *Macromolecules* **2006,** *39*, 3531-3539.

17. Aktas Eken, G.; Acar, M. H. PVDF-Based Shape Memory Polymers. *Eur. Polym. J.* **2019,** *114*, 249-254.

18. Sheiko, S. S.; Sumerlin, B. S.; Matyjaszewski, K. Cylindrical Molecular Brushes: Synthesis, Characterization, and Properties. *Prog. Polym. Sci.* **2008,** *33*, 759-785.

19. Feng, C.; Li, Y.; Yang, D.; Hu, J.; Zhang, X.; Huang, X. Well-Defined Graft Copolymers: from Controlled Synthesis to Multipurpose Applications. *Chem. Soc. Rev.* **2011,** *40*, 1282-1295.

20. Verduzco, R.; Li, X.; Pesek, S. L.; Stein, G. E. Structure, Function, Self-Assembly, and Applications of Bottlebrush Copolymers. *Chem. Soc. Rev.* **2015,** *44*, 2405-2420.

21. Neugebauer, D.; Zhang, Y.; Pakula, T.; Matyjaszewski, K. Heterografted PEO–P*n*BA Brush Copolymers. *Polymer* **2003,** *44*, 6863-6871.

22. Xie, G.; Krys, P.; Tilton, R. D.; Matyjaszewski, K. Heterografted Molecular Brushes as Stabilizers for Water-in-Oil Emulsions. *Macromolecules* **2017,** *50*, 2942-2950.

23. Tundo, P.; Selva, M. The Chemistry of Dimethyl Carbonate. *Acc. Chem. Res.* **2002,** *35*, 706-716.

24. Zhang, H.; Ruckenstein, E. Self-Polyaddition of Hydroxyalkyl Vinyl Ethers. *J. Polym. Sci., Part A: Polym. Chem.* **2000,** *38*, 3751-3760.

25. Hashimoto, T.; Ishizuka, K.; Umehara, A.; Kodaira, T. Synthesis of Polyacetals with Various Main-Chain Structures by the Self-Polyaddition of Vinyl Ethers with a Hydroxyl Function. *J. Polym. Sci., Part A: Polym. Chem.* **2002,** *40*, 4053-4064.

26. Sugihara, S.; Kawamoto, Y.; Maeda, Y. Direct Radical Polymerization of Vinyl Ethers: Reversible Addition–Fragmentation Chain Transfer Polymerization of Hydroxy-Functional Vinyl Ethers. *Macromolecules* **2016,** *49*, 1563-1574.

27. Valade, D.; Boschet, F.; Améduri, B. Synthesis and Modification of Alternating Copolymers Based on Vinyl Ethers, Chlorotrifluoroethylene, and Hexafluoropropylene. *Macromolecules* **2009,** *42*, 7689-7700.

28. Yamada, K.; Miyazaki, M.; Ohno, K.; Fukuda, T.; Minoda, M. Atom Transfer Radical Polymerization of Poly(vinyl ether) Macromonomers. *Macromolecules* **1999,** *32*, 290-293.

29. Bevington, J. C.; Hunt, B. J.; Jenkins, A. D. Effect of Vinyl Ethers upon Radical Polymerizations. *Pure Appl. Chem.* **2000**, *A37*, 609-619.

30. Santhosh Kumar, K. S.; Améduri, B. Synthesis and Characterization of Epoxy Functionalized Cooligomers Based on Chlorotrifluoroethylene and Allyl Glycidyl Ether. *J. Polym. Sci., Part A: Polym. Chem.* **2010,** *48*, 3587-3595.

31. Beers, K. L.; Gaynor, S. G.; Matyjaszewski, K.; Sheiko, S. S.; Möller, M. The Synthesis of Densely Grafted Copolymers by Atom Transfer Radical Polymerization. *Macromolecules* **1998**, *31*, 9413-9415.

32. Cheng, G.; Böker, A.; Zhang, M.; Krausch, G.; Müller, A. H. E. Amphiphilic Cylindrical Core-Shell Brushes via a “Grafting From” Process Using ATRP. *Macromolecules* **2001**, *34*, 6883-6888.

33. Puts, G.; Lopez, G.; Ono, T.; Crouse, P. Ameduri, B. Radical Copolymerization of Chlorotrifluoroethylene with Isobutyl Vinyl Ether Initiated by the Persistent Perfluoro-3-Ethyl-2,4-Dimethyl-3-Pentyl Radical. *RSC Adv.* **2015**, *5*, 41544-41554.

34. Ahn, N. Y.; Seo, M. Heteroarm Core Cross-Linked Star Polymers via RAFT Copolymerization of Styrene and Bismaleimide. *RSC Adv.* **2016,** *6*, 47715-47722.

35. Ahn, N. Y.; Seo, M. Synthetic Route-Dependent Intramolecular Segregation in Heteroarm Core Cross-Linked Star Polymers as Janus-Like Nanoobjects. *Polym. Chem.* **2020**, *11*, 449-460.

36. Seo, M.; Murphy, C. J.; Hillmyer, M. A. One-Step Synthesis of Cross-Linked Block Polymer Precursor to a Nanoporous Thermoset. *ACS Macro Lett.* **2013,** *2*, 617-620.

37. Oh, J.; Kim, B.; Lee, S.; Kim, S.-H.; Seo, M. Semipermeable Microcapsules with a Block-Polymer-Templated Nanoporous Membrane. *Chem. Mater.* **2018,** *30*, 273-279.

38. Voet, V. S. D.; Tichelaar, M.; Tanase, S.; Mittelmeijer-Hazeleger, M. C.; Ten Brinke, G.; Loos, K. Poly(vinylidene fluoride)/Nickel Nanocomposites from Semicrystalline Block Copolymer Precursors. *Nanoscale* **2013,** *5*, 184-192.

39. Voet, V. S. D.; Hermida-Merino, D.; Ten Brinke, G.; Loos, K. Block Copolymer Route Towards Poly(vinylidene fluoride)/Poly(methacrylic acid)/Nickel Nanocomposites. *RSC Adv.* **2013,** *3*, 7938-7946.

40. Rzayev, J.; Hillmyer, M. A. Nanochannel Array Plastics with Tailored Surface Chemistry. *J. Am. Chem. Soc.* **2005,** *127*, 13373-13379.

41. Seo, M.; Hillmyer, M. A. Reticulated Nanoporous Polymers by Controlled Polymerization-Induced Microphase Separation. *Science* **2012,** *336*, 1422.

42. McIntosh, L. D.; Schulze, M. W.; Irwin, M. T.; Hillmyer, M. A.; Lodge, T. P. Evolution of Morphology, Modulus, and Conductivity in Polymer Electrolytes Prepared via Polymerization-Induced Phase Separation. *Macromolecules* **2015,** *48*, 1418-1428.

43. Brunauer, S.; Emmett, P. H.; Teller, E. Adsorption of Gases in Multimolecular Layers. *J. Am. Chem. Soc.* **1938,** *60*, 309-319.

44. Barrett, E. P.; Joyner, L. G.; Halenda, P. P. The Determination of Pore Volume and Area Distributions in Porous Substances. I. Computations from Nitrogen Isotherms. *J. Am. Chem.*

Soc. **1951,** *73*, 373-380.

45. Cavicchi, K. A.; Zalusky, A. S.; Hillmyer, M. A.; Lodge, T. P. An Ordered Nanoporous Monolith from an Elastomeric Crosslinked Block Copolymer Precursor. *Macromol. Rapid Commun.* **2004,** *25*, 704-709.

46. Puts, G.; Venner, V.; Améduri, B.; Crouse, P. Conventional and RAFT Copolymerization of Tetrafluoroethylene with Isobutyl Vinyl Ether. *Macromolecules* **2018,** *51*, 6724-6739.